2.5 Gbit/s Data Transmission over 10 km Standard Single-Mode Fiber Using InGaAs VCSELs at 1.13 μm Emission Wavelength

Jürgen Joos and Irene Ecker

Vertical-cavity surface-emitting lasers with an InGaAs quantum well, operating at 1129 nm have been fabricated. Due to lateral single-mode behavior and narrow far-field angles the devices are versatile sources for optical fiber links. Bit error rates (BER) of less than 10^{-11} are demonstrated for 2.5 Gbit/s data transmission over 10 km standard single-mode fiber.

1. Introduction

Vertical-cavity surface-emitting lasers (VCSELs) with emission wavelengths beyond 1 μm are extremely attractive sources for long-distance optical communication. Even though there has been much effort in developing long-wavelength VCSELs there is much more success in fabricating high-performance near-infrared (850 nm and 980 nm) devices [1]. Nevertheless, there have been remarkable results in data transmission experiments using double-fused VCSELs [2, 3]. However, due to complicated processing this conception has lost importance with respect to new technologies of GaAs-based long-wavelength VCSELs. Recently there has been great success in fabricating devices with active materials including Sb [4], InAs quantum dots [5], and GaInNAs [6]. We present single-mode vertical-cavity lasers with a highly strained InGaAs quantum well emititing at 1129 nm wavelength, and demonstrate 2.5 Gbit/s data transmission over 10 km optical fiber.

2. Device fabrication

The VCSEL devices are grown by solid source molecular beam epitaxy. The active zone consists of a single 7 nm thick $In_{0.33}Ga_{0.67}As$ quantum well embedded between GaAs cladding layers. The quantum well thickness and composition is kept slightly below the critical thickness, calculated according to the Matthew-Blakeslee formula. The p-type and n-type AlGaAs-GaAs Bragg reflectors are doped using carbon and silicon, respectively. After epitaxial growth and wet chemical mesa etching, the current aperture with an active diameter of about 6 μm is defined. This is carried out by selective oxidation of an AlAs layer in a hot water vapor environment. Further fabrication steps are Ti-Pt-Au top metal contact evaporation, passivation layer deposition, Ge-Ni-Au bottom metal contact evaporation, bond pad deposition, and wire bonding. The device structure is shown in Fig. 1.

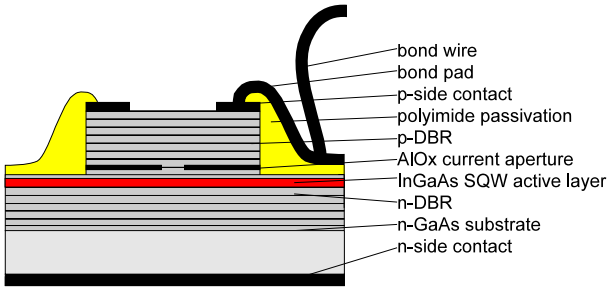

Fig. 1. Structure of a single InGaAs quantum well VCSEL

3. Device properties

In Fig. 2 and 3 the CW room temperature characteristics and the optical spectrum are depicted, respectively.

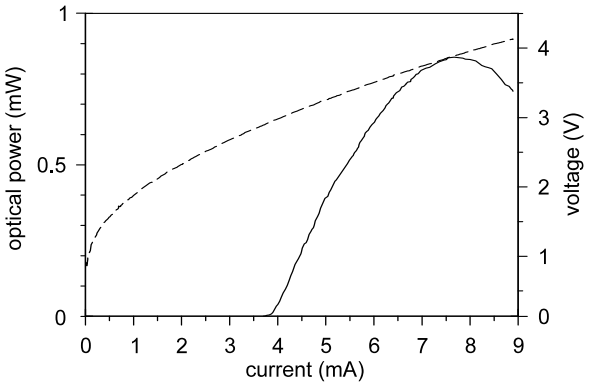

Fig. 2. Characteristics of 6 μm diameter long-wavelength InGaAs VCSEL

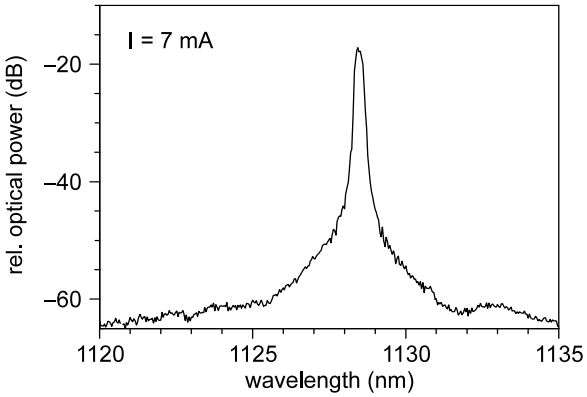

Fig. 3. CW emission spectrum of 6 μm diameter long-wavelength InGaAs VCSEL

The threshold current of the devices is 3.9 mA. While I-P-measurements were carried out using a large area photo detector, the spectrum was measured after butt-coupling into a 50 μm diameter fiber and exhibits transversal fundamental-mode emission at 1129 nm. Even beyond thermal rollover at about two times threshold current there is no visible side-mode. The peak width is limited by the resolution of the spectrum analyzer of 0.1 nm. Throughout the measurements the devices were not thermally mounted but simply attached to a copper carrier.

Fig. 4 shows the measured far field characteristics of the VCSEL and for comparison the far field of the standard single mode fiber used for data transmission experiments. Both of the far field measurements were carried out by recording the angular distribution of the optical power at a distance of 30 cm to the device. According to

$$2\Theta_{1/e} = \frac{2\lambda}{\pi w_0} \tag{1}$$

describing the relation between the $1/e^2$-width of the far field angle $\Theta_{1/e}$, the beam waist radius w_0, and the wavelength λ for Gaussian beams, the beam waist diameter was calculated to be 6.1 μm and therefore coincides very well with the active device diameter.

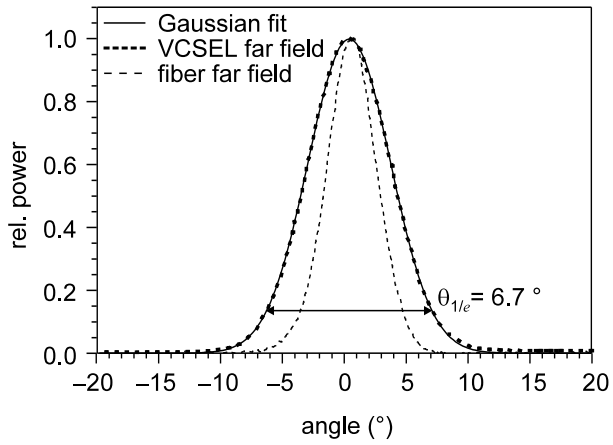

Fig. 4. Far field of 6 μm single-mode VCSEL and standard single-mode fiber.

Using the data from Fig. 4, the beam diameter of the fiber was calculated to be 10.2 μm. The output beam of the VCSEL reaches this value at a distance of 34 μm. This moderate beam widening allows coupling from the VCSEL into a standard single-mode fiber with measured efficiencies of greater than 90 %.

4. Dynamic properties

Fig. 5 shows RIN spectra measured at various bias currents. The RIN measurements were carried out by placing a $16\times16\,\mu\text{m}^2$ InGaAs photo diode directly in front of the laser device. Increasing current leads to decreasing noise not too far above the shot noise limit, which is located at -151 dB/Hz for a photo current of 375 μA, corresponding to 6.2 mA laser driving current. However, by further optimizing the threshold current density, a still lower noise, even below shot noise [7], could be expected. In order to describe the dynamic characteristics of the devices, the modulation efficiency has been examinated. The results are depicted in Fig. 6. From the slope of the fitting curve a modulation efficiency factor of $M_{\text{eff}} = 1.34\,\text{GHz/mA}^{1/2}$ has been extracted. After all emission wavelength has to be weighed against noise and RF characteristics of the devices.

Another measure of dynamic behavior, the so-called K-factor [8], is related to the intrinsic maximum 3 dB corner frequency by

$$\nu_{\max} = \sqrt{2}\frac{2\pi}{K}\,. \tag{2}$$

It is derived from its proportionality to the squared resonance frequency. According to Fig. 7 a K-factor of 2.51 ns was found, which corresponds to a corner frequency of $\nu_{\max} = 3.54\,\text{GHz}$.

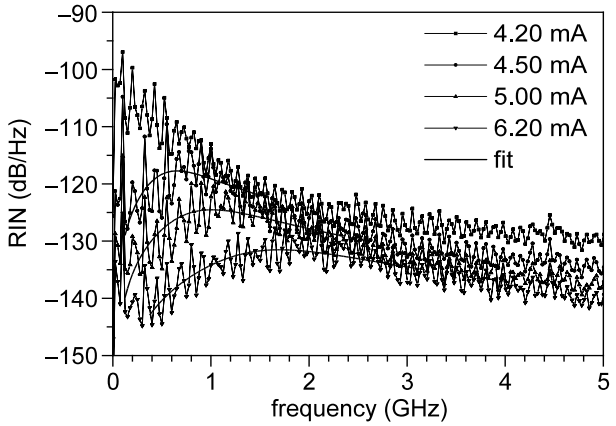

Fig. 5. VCSEL relative intensity noise for various bias currents.

The single quantum well as active layer is expected to be the reason for these moderate values. A large carrier density in the quantum well is required in order to provide sufficient gain, which in its turn leads to reduced differential gain $\partial g/\partial n$. However, by using two or more quantum wells the overall strain in the active region increases and the critical thickness could be exceeded.

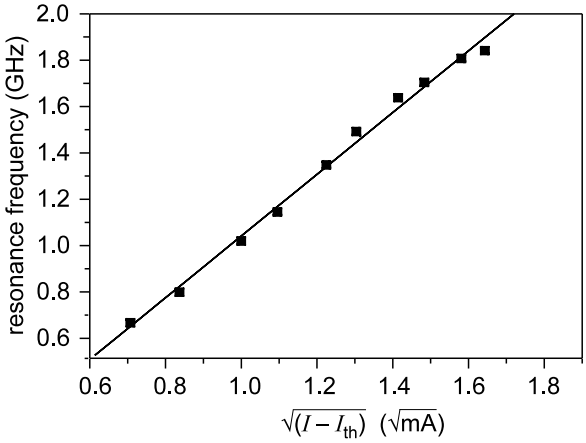

Fig. 6. Modulation efficiency.

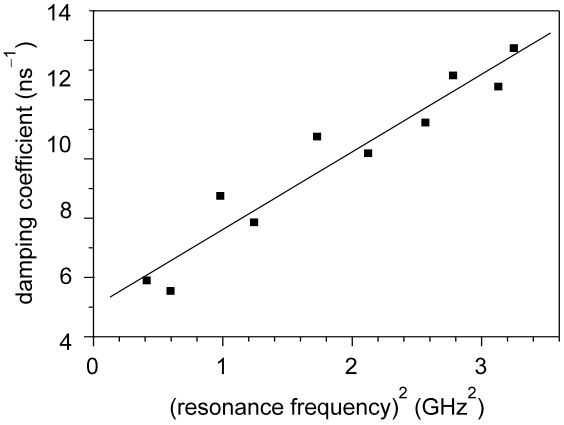

Fig. 7. Relation between damping coefficient and resonance frequency squared. The slope defines the K-factor.

5. Data transmission

Based on the preceding results, data transmission experiments were carried out. The device is driven at a bias current of 6 mA. A 2.5 Gbit/s pseudo-random bit sequence (PRBS) with $V_{pp} = 0.4$ V is added by means of a bias-tee. The reason for choosing this high bias current and hence the low modulation ectinction ratio is the increasing noise at lower currents, which

was approved by varying both of the values for optimum transmission results. The used word length of $2^7 - 1$ is standard for data encoding in LANs as e.g., Gigabit Ethernet using 8B/10B encoding. The optical signal passes a variable attenuator in order to adjust the optical power. It is detected by a 2 GHz bandwidth Ge pin-photo diode. The signal is monitored with an electrical sampling oscilloscope and analyzed with a BER decoder. The data transmission results are shown in Fig. 8 where open circles refer to back-to-back testing and plain diamonds denote transmission over 10 km standard single mode fiber. The comparatively low power penalty for 10 km transmission of 1 dB proofs the almost negligible amount of fiber dispersion. Thus, the limiting factor for going to distances larger than 10 km is absorption rather than dispersion. The eye diagram which was recorded at a bit-error rate of 10^{-11} is symmetric and wide open.

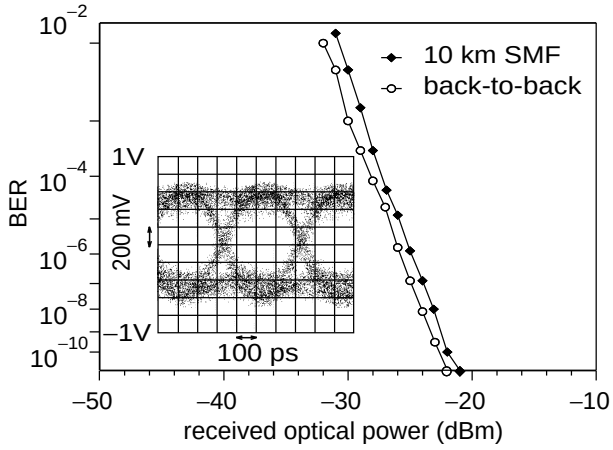

Fig. 8. Bit error rate (BER) characteristics for 2.5 Gbit/s data transmission over 10 km of standard single-mode fiber (SMF) and back-to-back testing. The inset eye diagram was recorded at BER $= 10^{-11}$.

6. Conclusion

We have demonstrated high-performance single-mode VCSELs with a single $In_{0.33}Ga_{0.67}As$ quantum well emitting at 1129 nm wavelength. The devices exhibit a far field angle of $\theta_{1/e} = 6.7\,^\circ$, an intrinsic corner frequency of 3.54 GHz, and a K-factor of 2.51 ns. Error-free data transmission was achieved with 2.5 Gbit/s PRBS over 10 km standard single-mode fiber.

Acknowledgments

This work is supported by the Volkswagen Stiftung which is gratefully acknowledged.

References

[1] D. Wiedenmann, R. King, C. Jung, R. Jäger, R. Michalzik, P. Schnitzer, M. Kicherer, and K.J. Ebeling "Design and analysis of single-mode oxidized VCSEL's for high-speed optical interconnects ", *IEEE J. Sel. Topics Quantum Electron.,* vol 5, pp 503-511, 1999

[2] S.Z. Zhang, N.M. Margalit, T.H. Reynolds, J.E. Bowers, "1.54-μm vertical-cavity surface-emitting laser transmission at 2.5 Gb/s", *IEEE Photon. Technol. Lett.,* vol. 9, pp. 374-376, 1997.

[3] V. Jayaraman, J.C. Geske, M.H. MacDougal, F.H. Peters, T.D. Lowes, and T.T. Char, "Uniform threshold current, continuous-wave, singlemode 1300nm vertical cavity lasers from 0 to 70 °C", *Electron. Lett.,* vol. 34, pp. 1405-1407, 1998

[4] T. Anan, M. Yamada, K. Tokutome, S. Sugou, K. Nishi, and A. Kamei, "Room-temperature pulsed operation of GaAsSb/GaAs vertical-cavity surface-emitting lasers", *Electron. Lett.*, vol. 35, pp. 903-904, 1999

[5] D.L. Huffaker, G. Park, Z. Zhou, O.B. Shchekin, D.G. Deppe, "1.3 μm room-temperature GaAs-based quantum-dot laser", *Appl. Phys. Lett.,* vol. 73, pp. 2564-2566, 1998

[6] K. Nakahara, M. Kondow, T. Kitatani, M.C. Larson, K. Uomi, "1.3-μm continuous-wave lasing operation in GaInNAs quantum-well lasers", *IEEE Photon. Technol. Lett.,* vol. 10, pp. 487-488, 1998

[7] D. Wiedenmann, P. Schnitzer, C. Jung, M. Grabherr, R. Jäger, R. Michalzik, K.J. Ebeling, "Noise characteristics of 850 nm single-mode vertical cavity surface emitting lasers", *Appl. Phys. Lett.,* vol. 73, pp. 717-719, 1998.

[8] R. Michalzik, R. King, D. Wiedenmann, P. Schnitzer, K.J. Ebeling, "Modeling and application of VCSELs for optical interconects", *Proc. Optoelectronics '99, Physics and simulation of optoelectronic devices VII,* vol. 3625, San Jose, California, USA, Jan., 1999.